

# Ignition and Unstable Regimes of Gasless Combustion of a Disk-Shaped Sample

V. G. Prokof'ev<sup>a</sup> and V. K. Smolyakov<sup>a,b</sup>

UDC 536.46

Published in *Fizika Goreniya i Vzryva*, Vol. 53, No. 1, pp. 43–47, January–February, 2017.  
Original article submitted February 6, 2016.

**Abstract:** The effect of ignition conditions and the parameters of the melting of the inert component on unstable combustion modes is studied numerically using a model of solid-flame combustion of a disk. It is shown that the shape of the heated region initiating combustion of the disk determines the number and trajectories of hotspots of the self-propagating combustion zone. The effect of the phase transition on the combustion characteristics is the more pronounced the closer the phase transition temperature to the combustion temperature. In this case, the combustion front takes the shape of a ring.

**Keywords:** gasless combustion, unstable combustion mode, phase transition.

**DOI:** 10.1134/S0010508217010063

## INTRODUCTION

One of the clearest manifestations of unstable propagation of solid-flame combustion are spin modes which are observed in cylindrical samples prepared from a mixture of solid components [1, 2]. In flat disk-shaped samples unstable combustion modes with hot spots moving along various paths, including spiral ones, occur [3, 4]. In [5], a numerical simulation of solid-flame combustion of a disk-shaped sample was performed and the combustion modes are classified according to the stability parameter of propagation of a flat front  $\alpha_{st} = 9.1Td - 2.5Ar$  [6], where  $Td$  and  $Ar$  are the Arrhenius and Todes parameters. For the establishment of the hot-spot combustion mode [5], asymmetric bending of the igniting pellet is proposed, but it is not indicated how this asymmetry is specified. Note that in experimental studies, hot-spot combustion modes of disk have been observed only in gasless systems with phase transformations and the formation of melts [3, 4].

In this work, combustion of a disk was studied using a two-dimensional solid-flame combustion model consid-

ering the melting of the inert component of the mixture. Ignition was initiated by a hot region in the center of the disk which corresponds to an igniting pellet in experiments. Critical ignition conditions were not considered. In [7], a similar problem of combustion with a stepwise change in the diameter of the cylindrical sample is solved and critical conditions for combustion-wave propagation were found as a function of the ratio of the diameters of the small and large cylinders.

The mathematical model of solid-flame combustion for two-dimensional unsteady combustion waves with melting of the inert component for a disk-shaped sample is written as follows:

$$[1 + Ph\delta(\theta - \theta_l)] \frac{\partial \theta}{\partial \tau} = \frac{1}{\xi} \frac{\partial}{\partial \xi} \left( \xi \frac{\partial \theta}{\partial \xi} \right) + \frac{1}{\xi^2} \frac{\partial^2 \theta}{\partial \varphi^2} + \frac{1}{Td} \frac{d\eta}{d\tau}, \quad (1)$$

$$\frac{d\eta}{d\tau} = Td(1 - \eta) \exp \frac{\theta}{1 + Ar\theta} \quad (2)$$

$(0 \leq \xi \leq R_0, \quad -\pi \leq \varphi \leq \pi);$

the boundary conditions are given by:

$$\tau = 0: \theta(\xi, \varphi, 0) = \theta_0, \eta(\xi, \varphi, 0) = 0 (M(\xi, \varphi) \notin S),$$

$$\eta(\xi, \varphi, 0) = 1 (M(\xi, \varphi) \in S),$$

$$0 < \tau < \tau_{\text{ign}}: \theta(M, \tau) = \theta_{\text{ign}} (M(\xi, \varphi) \in S),$$

<sup>a</sup>Tomsk State University, Tomsk, 630050 Russia.

<sup>b</sup>Department of Structural Macrokinetics, Siberian Branch, Russian Academy of Sciences, Tomsk, 634021 Russia; pvg@ftf.tsu.ru.

$$\xi = R_0: \frac{\partial \theta(R_0, \varphi, \tau)}{\partial \xi} = 0. \quad (3)$$

The dimensionless parameters and variables are

$$\begin{aligned} \text{Td} &= \frac{cRT_*^2}{QE}, \quad \theta = \frac{(T - T_*)E}{RT_*^2}, \quad \theta_l = \frac{(T_l - T_*)E}{RT_*^2}, \\ \theta_0 &= \frac{(T_0 - T_*)E}{RT_*^2}, \quad \text{Ar} = \frac{RT_*}{E}, \\ \xi &= \frac{r}{x_*}, \quad x_* = \sqrt{\frac{\lambda t_*}{c\rho}}, \quad t_* = \frac{cRT_*^2}{QEK(T_*)}, \quad \tau = \frac{t}{t_*}, \\ \tau_{\text{ign}} &= \frac{t_{\text{ign}}}{t_*}, \quad R_0 = \frac{R_S}{x_*}, \quad \text{Ph} = \frac{Q_l}{Q\text{Td}}. \end{aligned}$$

Here  $T$  is the temperature,  $T_* = T_0 + (Q - Q_l)/c$  is the adiabatic combustion temperature with heat consumption for melting the inert component,  $T_0$  is the initial temperature of melting of the sample,  $T_l$  is the melting temperature,  $c$  is the specific heat,  $Q$  is the heat of the reaction,  $Q_l$  is the melting heat per unit mass of the inert component,  $\rho$  is the density,  $t$  is time,  $r$  and  $\varphi$  are the radial and angular coordinates, respectively,  $T_{\text{ign}}$  and  $t_{\text{ign}}$  are the temperature and duration of the thermal pulse,  $S$  is the region affected by the thermal pulse,  $K(T)$  is the reaction rate constant,  $E$  is the activation energy,  $R_S$  is the radius of the disk,  $\delta(\theta - \theta_l)$  is the delta function,  $\text{Ph}$  is the relative heat of melting,  $\theta_l$  is the dimensionless melting temperature. The effect of the phase transition in the heat transfer is taken into account by introducing the effective heat capacity function  $c(\theta) = 1 + \text{Ph}\delta(\theta - \theta_l)$ . This method has been used to describe the effect of melting of the inert component on the propagation of a plane combustion wave [8]. To reduce the number of secondary parameters, we assume the equality of the thermal characteristics of all components of the system.

Problem (1)–(3) was solved by the a finite-difference method using an implicit scheme with constant steps along the coordinates and in time. Standard sweep was used along the radial coordinate, and a cyclic sweep along the angular coordinate. The basic values of the difference grid steps in the axial and radial coordinates and time were fixed equal to  $h = 0.25$  and  $\Delta\tau = 0.5$ , and for the angle,  $\Delta\varphi = 0.001\pi$ . In the numerical solution of Eq. (1), we used smoothing of the delta function:

$$\begin{aligned} \delta(\theta) &\approx \Phi(\theta) = \frac{\varphi(\theta)\text{erf}^{-1}(\sqrt{2})}{\Delta\theta\sqrt{2}\pi} \exp\left(-\frac{(\theta_l - \theta)^2}{2\Delta\theta^2}\right), \\ \varphi(\theta) &= \begin{cases} 0, & \theta > \theta_l + \Delta\theta, \\ 1, & \theta_l - \Delta\theta < \theta < \theta_l + \Delta\theta, \\ 0, & \theta < \theta_l - \Delta\theta. \end{cases} \end{aligned}$$

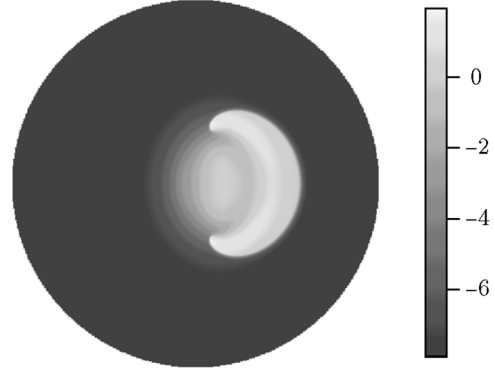


**Fig. 1.** Temperature field of the disk:  $\tau = 4836$ ,  $R_0 = 600$ ,  $\theta_0 = -8$ ,  $\text{Ar} = 0.11$ ,  $\theta_{\text{ign}} = 0$ ,  $\tau_{\text{ign}} = 4500$ , and  $\text{Ph} = 0$ .

The function  $\Phi(\theta)$  was subjected to the normalization condition  $\int_{\theta - \Delta\theta}^{\theta + \Delta\theta} \Phi(\theta)d\theta = 1$ , which does not depend on the smoothing interval  $\Delta\theta$ .

Note that infinitely thin flat samples do not exist. To validate the two-dimensional idealization of the problem, we performed calculations of the ignition and gasless combustion of a disk of finite thickness in a three-dimensional formulation with adiabatic boundary conditions along the axial coordinate  $z$ :

$$\frac{\partial \theta(\xi, \varphi, 0, \tau)}{\partial z} = 0, \quad \frac{\partial \theta(\xi, \varphi, h, \tau)}{\partial z} = 0.$$

The thickness of the disk in the selected scale is  $h = 20$ , which is far less than the radius of the disk  $R_0$ . The region  $S$  was an annular sector ( $50 < \xi < 150$  and  $|\varphi| < \pi/3$ ) on the face  $z = 0$ . In the three-dimensional case, the part of the disk which has a projection onto the region  $S$  was maintained at a temperature  $\theta_{\text{ign}}$  over the time interval  $\tau < \tau_{\text{ign}}$ . The temperature field at the time when the thermal pulse ( $\tau_{\text{ign}} = 4500$ ) ended is presented in the three-dimensional case in Fig. 1. The boundaries of the combustion region with two hot spots and the temperature distributions coincide up to 2% with the solution of the similar problem (1)–(3). However, in the two-dimensional case, the development the combustion zone ha a time delay  $\Delta\tau = 764$ , possibly due to the longer heating stage.

The ignition conditions (geometry and temperature of the region  $S$  and the duration of the thermal pulse  $\tau_{\text{ign}}$ ) determine the duration of the establishment of the mode and the type of combustion mode. The duration of the thermal pulse  $\tau_{\text{ign}}$  and the temperature  $\theta_{\text{ign}}$  in the region  $S$  must provide the establishment of self-propagating combustion of the disk. If the region  $S$  has

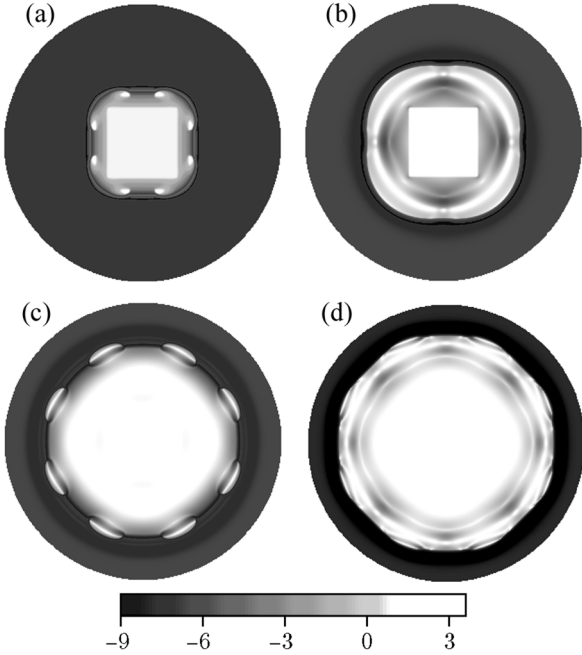


**Fig. 2.** Multi-hot-spot combustion mode for  $\tau = 926$  (a), 3691 (b), 5097 (c), and 5470 (d):  $\theta_{\text{ign}} = 1$ ,  $\tau_{\text{ign}} = 5000$ ;  $R_0 = 600$ ,  $\theta_0 = -9$ ,  $\text{Ar} = 0.08$ ,  $\text{Ph} = 0$ ; the igniting region  $S$  is a  $150 \times 150$  square.

the shape of a perfect circle with a uniform temperature distribution in it, the combustion zone is a circle expanding in time. To provide asymmetric propagation of the front with formation of hot spots moving along specific trajectories, we took the region  $S$  in the form of a square (Fig. 2), a semicircle (Fig. 3), and a non-uniformly heated circle (Fig. 4) while the stability parameter  $\alpha_{\text{st}}$  was considered to be fixed. The calculations showed the influence of the ignition conditions (geometry and size of the region  $S$ ) on the unstable combustion modes of the disk.

Temperature perturbations in the form of hotspots arise in the neighborhood of the corner points of the region  $S$ . Each of these points evolves into a pair of hot spots moving in opposite directions until meeting the hot spot moving from the neighboring vertex of the square (Fig. 2a). After merging, the hotspots form an annular front around the region  $S$  (Fig. 2b). The annular combustion front expands to form eight new hot spots (Fig. 2c), each of which form a nest new pair of hot spots moving in opposite directions on a circle of the same radius. At this time, the action of the thermal pulse ends and the temperature in the region of  $S$  begins to fall. Further merging of the hot spots leads to the formation of the next annular front with a more complex structure (Fig. 2d). At the time  $\tau = 5470$ , the total number of hot spots reaches 16, and they are arranged

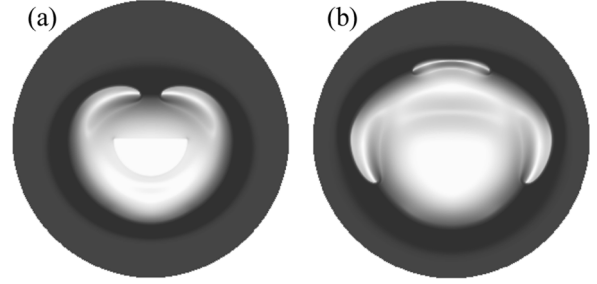


**Fig. 3.** Temperature field of the disk with the igniting region  $S$  in the form of a semicircle of radius  $|r| < 160$  ( $-\pi < \phi < 0$ ) for  $\tau = 4304$  (a) and 5580 (b):  $\theta_{\text{ign}} = 1$ ,  $\tau_{\text{ign}} = 5000$ ;  $R_0 = 600$ ,  $\theta_0 = -9$ ,  $\text{Ar} = 0.08$ , and  $\text{Ph} = 0$ .

on two concentric circles. In the final stage of the combustion, the temperature in the front is equalized, and all the points of the front move predominantly in radial direction to the boundary of the disk. Throughout the period of combustion of the disk, the temperature field is symmetric about the middle lines and diagonals of the square (the region  $S$ ), and the motion of the hot spots is ordered.

Note that in experiments where initiation is carried out by a wire or an igniting mixture, it is impossible to achieve perfect symmetry. Nevertheless, whatever the asymmetry of the geometry of the initiating region (pellet), the combustion zone tends to form a circle with high-temperature hot spots moving along its boundary. The hot spots move only in the region of instability of combustion-front propagation, and in the steady-state region, the circle becomes perfect over time. A departure from the symmetric motion of hot spots (randomization) begins at much larger disk sizes, several times exceeding the radius of the disk used in the work.

The development of the combustion zone in the region  $S$  in the form of a semicircle (Fig. 3) differs significantly from the above-described mode in Fig. 2. In the vicinity of the corner points of the region  $S$ , single hot spots are formed, which then move along the straight section of the boundary of the region  $S$  until merging into a single hot spot with a maximum temperature  $\theta_{\text{max}} = 3.7$ . Then, the next two hot spots are formed in this region, which move in opposite directions along a path of greater radius along the circular part of the boundary of the region  $S$ . During the motion, the maximum temperature increases from  $\theta_{\text{max}} = 2.9$  at the time  $\tau = 4685$  to  $\theta_{\text{max}} = 3.7$  at the time  $\tau = 5580$  and the areas of the hot spots, determined by the points with the temperature  $\theta > \theta_{\text{ign}}$ , increases by several times. The next pair of hot spots of moving along the path of greater radius are also formed on the axis of symmetry (Fig. 3b). This leads to rounding of the combustion

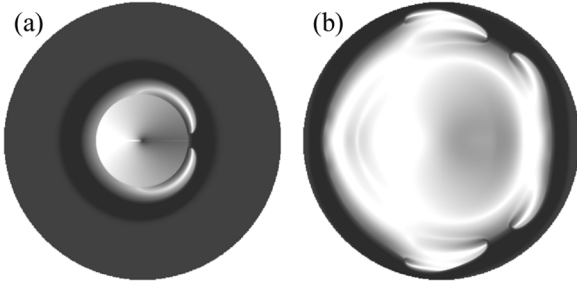


**Fig. 4.** Temperature field of the disk with the igniting region  $S$  in the form of a nonuniformly heated circle of radius  $|r| < 200$  for  $\tau = 1468$  (a) and  $6537$  (b):  $\theta_{\text{ign}} = \theta_0(\pi - |\varphi|)/2\pi + 1$ ,  $\tau_{\text{ign}} = 5000$ ,  $R_0 = 600$ ,  $\theta_0 = -9$ ,  $\text{Ar} = 0.08$ , and  $\text{Ph} = 0$ .



**Fig. 5.** Stabilization of the combustion wave: the igniting region  $S$  is a semicircle ( $|r| < 160$  and  $\pi < \varphi < 0$ ):  $\theta_{\text{ign}} = 1$ ,  $\tau_{\text{ign}} = 4500$ ;  $R_0 = 600$ ,  $\theta_0 = -9$ ,  $\text{Ar} = 0.08$ ,  $\text{Ph} = 0.4$ ,  $\theta_l = -0.5$ , and  $\tau = 4157$ .

front against the plane boundary of the region  $S$ . The temperature field is symmetric about the symmetry axis of the semicircle throughout the combustion of the disk. The initiation of combustion by a high-temperature region  $S$  in the form of a non-uniformly heated circle and the disk combustion mode are shown in Fig. 4. A feature of this regime is the formation of two opposing hot spots moving on trajectories of different radii (Fig. 4b). Note that all described modes have the following property: irrespective of the form of the region  $S$ , the combustion zone tends to assume the shape of a circle, which has the maximum area among all the figure with a fixed length of the boundary. The strongest temperature field perturbation arise at the corner points of the boundary of  $S$ , which leads to occurrence and development of hot spots in the neighborhood of these points.

The effect of the phase transition on the combustion is manifested through the melting heat and temperature  $\theta_l$  of the inert component of the mixture, which are then considered only as parameters of the problem.



**Fig. 6.** Effect of the phase transition on the multi-hot-spot combustion mode (the igniting region  $S$  is a  $150 \times 150$  square):  $\theta_{\text{ign}} = 1$ ,  $\tau_{\text{ign}} = 5000$ ;  $R_0 = 600$ ,  $\theta_0 = -9$ ,  $\text{Ar} = 0.08$ ,  $\text{Ph} = 0.3$ ,  $\theta_l = -1.5$ , and  $\tau = 5100$ .

The heat loss due to melting, defined by the parameter  $\text{Ph}$ , were compensated by the corresponding change in the thermal effect of the reaction due to a change in the Todes parameter  $\text{Td} = (\text{Ph} - \theta_0)^{-1}$ , which allowed the adiabatic combustion temperature to be considered constant at different melting heats.

The high-temperature phase transition  $-1 < \theta_l < 0$ , where the melting temperature is close to the adiabatic combustion temperature of a gasless mixture, leads to a complete stabilization of the combustion wave (Fig. 5), as in the one-dimensional case [8]. Possible development of hot spots with temperature exceeding the combustion temperature, is prevented by the phase transition. The combustion zone takes the form of a perfect circle (the region  $S$  has the form of a semicircle) with the temperature in the front  $\theta_f \approx \theta_l$ . At lower melting points, hot spots appear, whose number is determined by the configuration of the region  $S$ . The trajectories of the hot spots differ from the similar version with  $\text{Ph} = 0$ . Thus, during the initiation of the process by the region  $S$  in the form of a square, the combustion front contains straight sections, and the corresponding trajectories of the hot spot are parallel to the sides of the square (Fig. 6). The effect of the phase transition is manifested in that the region  $S$  retains its geometric shape for a longer time during combustion-wave propagation.

Summarizing the main results, we can draw the following conclusions.

1. The geometry of the igniting region  $S$ , along with the stability parameter  $\alpha_{\text{st}}$ , determines the combustion mode and its characteristics—the configuration of the front and features of motion of hot spots.

2. The number of hot spots in the initial stage of combustion of the disk is determined by the number of corner points of the boundary of the igniting region  $S$ .

3. The combustion zone tends to form a circle over time, regardless of the configuration of the region  $S$ .

4. The effect of the phase transition on the combustion characteristics is the stronger the nearer the phase-transition temperature to the combustion temperature and the greater the melting heat. In the limiting case where the melting temperature is close to the adiabatic combustion temperature, the combustion region quickly takes the form of a circle.

5. The effect of the low-temperature phase transition is manifested in the longer-term preservation of the geometric shape of the region  $S$  during combustion-wave propagation.

6. It is found that if the igniting region has symmetry, the symmetry manifests itself in the path of motion of the hot spots until the combustion zone reaches the boundary of the disk.

The work was supported by the Ministry of Education and Science of the Russian Federation (State Task No. 10.1329.2014/K).

## REFERENCES

1. Yu. M. Maksimov, A. G. Merzhanov, A. T. Pak, and M. N. Kuchkin, "Unstable Combustion Modes of Gasless Systems," *Fiz. Goreniya Vzryva* **17** (4), 51–58 (1981) [*Combust., Expl., Shock Waves* **17** (4), 393–400 (1981)].
2. Yu. M. Maksimov, A. T. Pak, G. B. Lavrenchuk, Yu. S. Naiborodenko, and A. G. Merzhanov, "Spin Combustion of Gasless Systems," *Fiz. Goreniya Vzryva* **15** (3), 156–159 (1979) [*Combust., Expl., Shock Waves* **15** (3), 415–418 (1979)].
3. A. G. Merzhanov, A. V. Dvoryankin, and A. G. Strunina, "A New Kind of Spin Combustion," *Dokl. Akad. Nauk SSSR* **267** (4), 869–872 (1982).
4. Yu. M. Maksimov and O. V. Lapshin, "Unstable Combustion of Flat Samples of the  $Ti + 2B + \alpha Cu$  System," *Khim. Fiz.* **34** (11), 50–54 (2015).
5. T. P. Ivleva, "Unsteady Solid-Flame Combustion Modes of a Disk," *Dokl. Akad. Nauk* **394** (4), 489–493 (2004).
6. K. G. Shkadinskii, B. I. Khaikin, and A. G. Merzhanov, "Propagation of a Pulsating Exothermic Reaction Front in the Condensed Phase," *Fiz. Goreniya Vzryva* **7** (1), 19–28 (1971) [*Combust., Expl., Shock Waves* **7** (1), 15–22 (1971)].
7. A. V. Pisklov, V. G. Prokof'ev, and V. K. Smolyakov, "Solid Flame Combustion of Cylindrical Samples with Stepwise Varying Diameter," *Fiz. Goreniya Vzryva* **45** (6), 26–30 (2009) [*Combust., Expl., Shock Waves* **45** (6), 657–661 (2009)].
8. V. G. Prokof'ev and V. K. Smolyakov, "Unsteady Combustion Regimes of Gasless Systems with a Low-Melting Inert Component," *Fiz. Goreniya Vzryva* **38** (2), 21–25 (2002) [*Combust., Expl., Shock Waves* **38** (2), 143–147 (2002)].